Jestr

Journal of Engineering Science and Technology Review 15 (3) (2022) 1 - 8

JOURNAL OF
Engineering Science and Technology Review

Research Article

www.jestr.org

Investigation On GFDM System For 5G Applications Over Fading Channels

Lingaiah Jada* and S.Shiyamala

School of Electrical and Communication Engineering | ECE, Vel Tech Rangarajan Dr.Sagunthala R&D Institute of Science and Technology, Avadi,Chennai-600 062,Tamilnadu,India

Received 22 February 2022; Accepted 20 July 2022

Abstract

The main goal of this paper is to investigate a generalized frequency division multiplexing (GFDM) system in Rician and Weibull fading settings utilizing the maximal ratio transmission (MRT) scheme.Now a day, most communication devices require low latency and low consumption of energy. In the literature, various multicarrier techniques are addressed and GFDM is one such technique that is new formulation research for future generations of mobile services. One of the major advantages of the GFDM technique is low out-of-band radiation. This paper initially explores the symbol error rate (SER) expression analysis in Rician and Weibull fading using the proposed GFDM-MRT system. Later on, performance is evaluated with MATLAB simulations for various simulation parameters such as the number of transmitting antennas, different roll-off factors, and various fading parameters. The performance is improved by 8dB to achieve the symbol error rate of 0.01 when we use the number of transmitting antennas ($N_t = 4$) compared to a single antenna($N_t = 1$). Finally, it can be concluded that GFDM-MRT techniques are more reliable for high-speed communications.

Keywords: GFDM, Maximal Ratio Transmission, symbol error rate, Rician fading, Weibull Fading, 5G network.

1.Introduction

It is expected that the 5G cellular networks of fifth-generation will tackle several things at a time to meet user's satisfaction. To meet their expectations, 5G systems require very little latency for the tactile internet, a loose synchronization for the Internet of Things (IoT), reliability, efficient and robust high throughput to communicate via bit pipe communication, large coverage area, and a dynamic allocation of the spectrum with the low value of out of band emission. The main factor that distinguishes between GFDM and OFDM is that number of subcarriers are non-orthogonal to each other in GFDM [1]. One more major advantage with GFDM is that cyclic prefixes (CP) are not added to each subcarrier so a lot of bandwidth is saved. In GFDM, only one CP is added to the combination of subcarriers, hence, we receive the same bits at the receiver that are transmitted from the transmitter. For carrier aggregation, OFDM was having a high Out of Band (OOB) emission and it is low for GFDM [2]. GFDM system is less complex, achieves low OOB and it is promising 5G solution is stated in [3-4]. In [5], the authors discussed that GFDM is a flexible technology that overcomes the drawbacks presented in 4G technology. As a result, it suggests that GFDM is backward compatible with long-term evolution's accumulated knowledge.

The OOB emission of GFDM can be reduced if there is a smooth transition between the blocks of GFDM. The guard band is used in between the GFDM blocks by erasing the first sub-symbol and there will be the orientation of signal edges towards zero corresponding to that. This makes the transition between the blocks of GFDM smooth. This whole process is named guard-symbol GFDM (GS-GFDM) [6]. Generally, GFDM is a waveform that is non-orthogonal but it can be made orthogonal by using various pulse shaping filters. It can also be done by making use of the combination of GFDM and orthogonal quadrature amplitude modulation (OQAM).

GFDM is a less complex approach, it can implement an LTE master clock for 5G Physical layers. Along with that the time-frequency structure of the nowadays cellular systems can also be implemented in [7]. Various circular pulse shaping filters are addressed in [8-10] which are used in the GFDM system to meet the requirements in the latest technologies. The GFDM signal is generated by multiplying and concatenating input symbols with an appropriate prototype filter [11].

ISI can be removed but noise value is enhanced using a zero forced (ZF) receiver. Further, the efficiency of the GFDM receiver can be increased with a minimum mean square estimation (MMSE) receiver [12]. ICI reduction approaches are suggested in [13]. A pre-coded GFDM system is discussed in [14]. To minimize ICI and the complexity of the receiver, the scheme was suggested in [14]. In [11], GFDM, OFDM, and single carrier frequency division (SC-FDM) analysis and their PAPRs performances were compared and it stated that GFDM achieves lower PAPR. The symbol error rate (SER) expression over the AWGN channel for the GFDM system with a ZF receiver is shown in [5].

The multiple-input and multiple-output (MIMO) based GFDM analysis is described in [15-16] which receiver complexity is more. This method uses a maximal ratio combining (MRC) scheme before demodulation. A large-scale MIMO transmission GFDM scheme is described in [17]. In [18], V-BLAST and spatial modulation schemes are used in the GFDM system and bit error rate (BER) performance is evaluated. The complexity of identification of MIMO-GFDM signals analysis is given in [19]. The detection complexity is further reduced in the MIMO-

*E-mail address: jadalingaiah69@gmail.com
ISSN: 1791-2377
doi:10.25103/jestr.153.01

GFDM system using the Montecarlo algorithm in [20-21]. MIMO structure and MRT also reduces the complexity in [22-23]. Weibull fading is a basic statistical model that can be used in both indoor and outdoor settings, according to studies [31]. The importance of the Weibull fading channel in digital modulation systems is convincingly demonstrated in [32]. Some detailed analysis about the Weibull fading channel is provided in [33].

With the use of Maximal ratio transmission (MRT), receiver complexity in MIMO systems is reduced. There is not much work is addressed in the literature related to GFDM with MRT. The MRT-based GFDM system performance is evaluated over Nakagami-*m* fading channel in [24]. The above-stated references are useful to analyze the performance of GFDM with the MRT scheme in the Rician fading channel.

The remaining paper is structured in other four sections. The proposed GFDM based MRT scheme is described in section-2. Section-3 deals with the SER analysis in Rician and Weibull fading. Simulation analysis followed by conclusions is given in section-4 and section-5 respectively.

2. System Model Description

The proposed GFDM based MRT system model is shown in Fig. 1. The proposed system is having a transmitter and receiver. The transmitter consists of an encoder, mapper, and other various blocks. The vectorial data $(\boldsymbol{b})$in the form of bits given as input to the encoder. The encoder converts the input from low bit-rate data stream into high bit-rate data stream and the output of the data vector is $(\boldsymbol{b_c})$. The output of the encoder is given as input to the mapper and it produces output as $N\ X\ 1$ data vector $(\boldsymbol{d})$. This vectorial data is given as input to the GFDM modulator which consists of N elements. The vectorial data $(\boldsymbol{d})$ is decomposes into $\boldsymbol{K}$ groups $\boldsymbol{M}$ symbols as follows.

$$d = [(d_0)^T, (d_1)^T, \dots \dots (d_{K-1})^T]^T \quad (1)$$

with

$$d_k = \left[d_{k,0}, d_{k,1}, \dots \dots d_{k,M-1}\right]^T \quad (2)$$

In eq, (2), $d_{k,m}$ is data symbol which is transmitted through *k*-th subcarrier at *m*-th time slot and $\boldsymbol{g_{k,m}}(\boldsymbol{n})$is filter coefficient. Let us assume that the GFDM block occupies $\boldsymbol{K}$ subcarriers, each subcarrier consists of $\boldsymbol{M}$ data symbols and it produces $\boldsymbol{N} = \boldsymbol{KM}$ samples. With GFDM modulator, samples are filtered with a corresponding transmit filter is given as [11]

$$g_{k,m}[n] = g[(n - mk) mod N] e^{\frac{-j2\pi kn}{K}} \quad (3)$$

The exponential term conducts frequency domain shift, and $g_{k,m}$ (n) is a time and frequency shifted version of g (n). Finally, all the transmitted symbols are superimposed at one place that leads to GFDM signal which is given as $\boldsymbol{x}(\boldsymbol{n})$in [11]

$$x[n] = \sum_{k=0}^{K-1} \sum_{m=0}^{M-1} d_{k,m} g_{k,m}[n],\ n = 0,1 \dots \dots KM - 1 \quad (4)$$

The pulse-shaping filter samples can be shown as follows

$$g_{k,m} = \left[g_{k,m}[0], g_{k,m}[1] \dots \dots g_{k,m}[MK-1]\right]^T \quad (5)$$

and matrix representation of eq. (4) is [12]

$$x = Ad \quad (6)$$

where $\boldsymbol{A}$ is a $\boldsymbol{KM\ X\ KM}$ dimension matrix which is also known as GFDM modulation matrix and is represented as [5]

$$A = \left[g_{0,0} \cdots g_{K-1,0} g_{0,1} \cdots g_{K-1,M-1}\right] \quad (7)$$

A cyclic prefix (CP) and cyclic suffix (CS) are added after GFDM block and then signal components are weighted with MRT coefficients as;

$$x_i = w_i x \quad (8)$$

where w_i is weighting factor (MRT coefficient) for *i*-th antenna and $(i = 1,2 \dots . N_t)$ [22];

$$w_i = \frac{h_i^*}{h_F} \quad (9)$$

$$h_F = \|h\| = \sqrt{\sum_{i=1}^{N_t} |h_i|^2}$$

In eq. (9), h_i is channel coefficient. h_F Frobenius norm of channel vector $h = \left[h_1, h_2 \dots h_{N_t}\right]$.

Finally, the GFDM signal is multiplied with MRT coefficients is received at the receiver and its mathematical representation is

$$r = \sqrt{P_t} \sum_{i=0}^{N_t} h_i w_i x + w = \sqrt{P_t} h_F x + w \quad (10)$$

Where **w** is a noise vector $w \sim (0,\ \sigma_w^2)$. Later on, power is normalized by $P_t = 1/N_t$ at each antenna, so that channel coefficient in eq. (9) is equalized. Finally, an output signal from the equalizer is demodulated by matched filter (MF), ZF, and MMSE. The expression for the demodulated signal is [5]

$$\hat{d} = By \quad (11)$$

where $\boldsymbol{B}$ is a demodulation matrix.

The demodulation matrix for the MF receiver is $B_{MF} = A^H$ which maximizes SNR and self-interference. Likely, for MMSE receiver $\boldsymbol{B}$ matrix is

$$B_{MMSE} = (R_n^2 + A^H H^H A H)^{-1} A^H H^H$$

which balances self-interference and noise enhancement and R_n^2 is the noise covariance matrix. Similarly, the $\boldsymbol{B}$ matrix for the ZF receiver is $B_{MF} = A^{-1}$. While the ZF receiver eliminates self-interference, it significantly improves noise efficiency.

The noise enhancement factor (NEF) 'ξ' represents the amount of reduction in SNR value when uses ZF receiver and its mathematical expression is [5]

$$\xi = \sum_{i=0}^{MK-1} \left|[B_{ZF}]_{k,i}\right|^2 \quad (12)$$

where'ξ' is equal for all $k = 0,1, \ldots . MK - 1$.

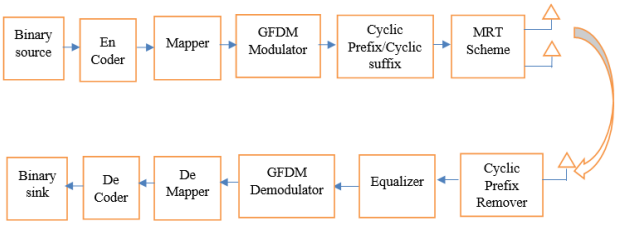

Fig. 1. Proposed GFDM Transceiver with MRT Scheme.

3. Symbol Error Rate Analysis

This section gives the analysis of GFDM based MRT scheme SER performance with ZF receiver in Rician and weibull fading environment. The usage of the ZF receiver in the proposed system reduces the self-interference but increases the noise value. The SER performance is evaluated using the QAM modulation scheme in the Rician and weibull channel. The channel impulse response of length N_{ch} can be represented as

$$h = [h_0, \ldots \ldots h_{Nch-1}]^T \tag{13}$$

The received signal mathematical representation at the receiver is

$$r = Hx + w \tag{14}$$

In the above expression r and x are received and transmitted information respectively. Where $\boldsymbol{H} = circ\{\bar{h}\}$ and $\bar{h}$ is a zero-padded version of h of the same length. For AWGN environment $\boldsymbol{H}$=**I**, where I is identity matrix. For the different fading environments in the wireless channel, $\boldsymbol{H}$ value varies. In this paper, we are considering Rician and weibull fading in the wireless channel since it can be modeled as most of the cases because it consists of a line of sight (LOS) component.

3.1. Rician Channel Model

The Rician channel can be modeled if the signal amplitude in the wireless channel follows the Rician distribution. The envelopes of channel coefficients are $|h_i|$ for $i = 1, 2, \cdots N_t$ and PDF is given as [27].

$$f_{|h_i|}(|h_i|) = \left(\frac{1+K}{\overline{h_i}}\right) exp\left[-\frac{(1+K)h_i + K\overline{h_i}}{\overline{h_i}}\right] I_0\left[\sqrt{\frac{4K(1+K)h_i}{\overline{h_i}}}\right]; \quad 0 \le K < \infty \tag{15}$$

Where K is the Rician fading parameter

The instantaneous SNR value is

$$\gamma = \frac{P_t E_s}{\xi N_0} h_F^2 \tag{16}$$

In eq. (16), $E_s$and N_0 are average energy per symbol and noise power spectral density respectively. From eq. (9), the envelope of $h_F$can be computed as

$$h_F = \sqrt{X_1^2 + X_2^2 + \ldots . + X_{2mN_t}^2} \tag{17}$$

where$X_i \sim (0, \sigma_X^2)$ and $(i = 1,2, \ldots 2mN_t)$ and $\widehat{K} = KN_t$[25], then the expression for PDF is

$$p_{h_F}(h_F) = \left(\frac{1+\widehat{K}}{\overline{h_F}}\right) exp\left[-\frac{(1+\widehat{K})h_F + \widehat{K}\overline{h_F}}{\overline{h_F}}\right] I_0\left[\sqrt{\frac{4\widehat{K}(1+\widehat{K})h_F}{\overline{h_F}}}\right]; \quad 0 \le K < \infty \tag{18}$$

Then, the PDF in terms of SNRs is given in [26];

$$p_\gamma(\gamma) = \left(\frac{1+\widehat{K}}{\overline{\gamma}}\right) exp\left[-\frac{(1+\widehat{K})\gamma + \widehat{K}\overline{\gamma}}{\overline{\gamma}}\right] I_0\left[\sqrt{\frac{4\widehat{K}(1+\widehat{K})\gamma}{\overline{\gamma}}}\right]; \quad 0 \le K < \infty \tag{19}$$

where $\overline{\gamma}$ is the average SNR value or $\bar{\gamma} = E[\gamma]$.

3.2 . SER of GFDM-MRT

This section gives the exact expressions of SER of the GFDM-MRT system over the non-fading environment ,Rician and weibull fading environment.

3.3 Non-fading (AWGN) Environment

The SNR is equally adjusted by NEF for GFDM at the receiver side. Hence, both OFDM SER and GFDM SER expressions for the AWGN environment are almost the same and they are differed in equivalent SNR [28]. The expression for SER under AWGN using GFDM system is [5];

$$P_{SER,AWGN}(\gamma) = 2\left(\frac{p-1}{p}\right) erfc(\sqrt{\gamma}) - \left(\frac{p-1}{p}\right)^2 erfc^2(\sqrt{\gamma}) \tag{20}$$

Where

$$\gamma = \frac{3R_T}{2(2^\mu - 1)} \frac{E_s}{\xi N_0} \; and_T = \frac{NM}{NM + N_{CP} + N_{CS}} \tag{21}$$

In eq. (20) and (21), $p = \sqrt{2\mu}$, μ represents the number of bits, N_{CP}, N_{Cs} are the length of CP and CS respectively. N and M are number of subcarriers and sub-symbols.

The SER expression for different fading environments can be evaluated by averaging the error rates AWGN over PDF of other fading channels. It can be calculated using [5]

$$P_{SER} = \int_0^\infty P_{AWGN}(\gamma)\, P_\gamma(\gamma) d\gamma \tag{22}$$

In eq. (22), $P_\gamma(\gamma)$ represents the PDF of different fading channels.

3.4 Rician Fading Environment

To calculate SER expression in Rician fading, we require a PDF of Rician fading. The PDF expression is shown in eq. (19), it can be further modified by expressing it in infinite series form of a zeroth model of Bessel function [29];

$$\boldsymbol{I_0(x)} = \sum_{q=0}^{\infty} \frac{\left(\frac{x^2}{4}\right)^q}{(q!)^2} \tag{23}$$

The modified PDF expression for the Rician fading environment is given in [25]

$$P_\gamma(\gamma) = \frac{1+K}{\overline{\gamma}_r} e^{-K} \sum_{q=0}^{\infty} \frac{1}{(q!)^2} \left(\frac{K(1+K)}{\overline{\gamma}_r}\right)^q \gamma^q \, exp\left(-\frac{\gamma(1+K)}{\overline{\gamma}_r}\right) \quad 0 \le K < \infty \tag{24}$$

Now, SER expression for Rician fading can be computed by substituting eq. (20) and eq. (24) in eq. (22), the bounded SER expression for GFDM system with single antenna is [25];

$$P_{SER,Ric}(\gamma) = \frac{2(p-1)}{p} I_3(\overline{\gamma}_r) - \left(\frac{p-1}{p}\right)^2 I_4(\overline{\gamma}_r) \tag{25}$$

Where $I_3(\overline{\gamma}_r)$and$I_4(\overline{\gamma}_r)$ are expressed as given below;

$$I_3(\overline{\gamma}_r) = \frac{1+K}{\overline{\gamma}_r} e^{-K} \sum_{q=0}^{\infty} \frac{1}{(q!)^2} \left(\frac{K(1+K)}{\overline{\gamma}_r}\right)^q \frac{\Gamma\left(q+\frac{3}{2}\right)}{\sqrt{\pi}(q+1)} \, {}_2F_1\left[q+1, q+\frac{3}{2}; q+2; +\left(\frac{1+K}{\overline{\gamma}_r}\right)\right] \tag{26}$$

$$I_4(\overline{\gamma}_r) = e^{-K} \sum_{q=0}^{\infty} \frac{K^q}{(q!)} \left(1 - \frac{4}{\Pi} \sum_{j=0}^{q} \frac{\left(\frac{(1+K)}{\overline{\gamma}_r}\right)^j}{2j+1} \, {}_2F_1\left[j+\frac{1}{2}, j+1; j+\frac{3}{2}; -\left(\frac{1+K}{\overline{\gamma}_r}+1\right)\right]\right) \tag{27}$$

Similarly, for multiple antennas (N_t) case, SER expression for GFDM based MRT system is obtained by changing $K$to KN_t, the bounded SER expression for GFDM based MRT system with multiple antennas is

$$P_{SER,Ric}(\gamma) = \frac{2(p-1)}{p} I_3(\overline{\gamma}_r) - \left(\frac{p-1}{p}\right)^2 I_4(\overline{\gamma}_r) \tag{28}$$

$$I_3(\overline{\gamma}_r) = \frac{1+KN_t}{\overline{\gamma}_r} e^{-K} \sum_{q=0}^{\infty} \frac{1}{(q!)^2} \left(\frac{N_t K(1+KN_t)}{\overline{\gamma}_r}\right)^q \frac{\Gamma\left(q+\frac{3}{2}\right)}{\sqrt{\pi}(q+1)} \, {}_2F_1\left[q+1, q+\frac{3}{2}; q+2; +\left(\frac{1+KN_t}{\overline{\gamma}_r}\right)\right] \tag{29}$$

$$I_4(\overline{\gamma}_r) = e^{-KN_t} \sum_{q=0}^{\infty} \frac{(KN_t)^q}{(q!)} \left(1 - \frac{4}{\Pi} \sum_{j=0}^{q} \frac{\left(\frac{(1+KN_t)}{\overline{\gamma}_r}\right)^j}{2j+1} \, {}_2F_1\left[j+\frac{1}{2}, j+1; j+\frac{3}{2}; -\left(\frac{1+KN_t}{\overline{\gamma}_r}+1\right)\right]\right) \tag{30}$$

where

$$\overline{\gamma}_r = \frac{3R_T\sigma_r^2}{(2^\mu-1)} \frac{E_s}{\xi N_0} \tag{31}$$

In the above eq. (31), $\bar{\gamma}_r$ is equivalent SNR in a Rician fading environment. Where ${}_2F_1[.,.;.;]$denotes the Gauss hypergeometric function [30]. It is assumed that σ_r^2 value is 0.5. If we substitute K = 0 for both single and multiple antennas cases, the expressions give the SER expressions for the Rayleigh fading environment. For K = 0, our simulation (Fig.2, black line) is exactly matching with the simulation (Fig.6, curve (i)) given in [25]. For $N_t = 1$, eq. (25) and eq. (28) are exactly match with each other.

4 Nakagami-*m* Fading Environment

The PDF expression for Nakagami-m fading environment is given in [24] as

$$p_\gamma(\gamma) = \left(\frac{m}{\overline{\gamma}}\right)^m \frac{\gamma^{m-1}}{\Gamma(m)} e^{-\frac{m\gamma}{\overline{\gamma}}} \tag{32}$$

To calculate SER expression in Nakagami-*m* fading, we require a PDF of Nakagami-*m* fading which is shown in eq. (32). Now, SER expression for Nakagami-*m* fading can be calculated by substituting equ. (20) and equ. (32) in equ. (22), the bounded SER expression for GFDM system with single antenna is given in [24];

$$P_{SER,Nak} = 2C_1 C_2^m \frac{\Gamma\left(m+\frac{1}{2}\right)}{\sqrt{\pi}\Gamma(m+1)} \, {}_2F_1\left[m, m+\frac{1}{2}; m+1; -C_2\right] - C_1^2\left[1 - \frac{4}{\pi}\sum_{j=0}^{m-1} \frac{C_2^j}{2j+1} \, {}_2F_1\left[j+\frac{1}{2}, j+1; j+\frac{3}{2}; -(C_2+1)\right]\right] \tag{33}$$

where C_1 and C_2 are expressed as follows;

$$C_1 = \frac{\sqrt{2^\mu}-1}{\sqrt{2^\mu}}, \quad C_2 = \frac{m}{\overline{\gamma}_n} \tag{34}$$

Similarly, for multiple antennas (N_t) case, SER expression for GFDM based MRT system is obtained by changing m to mN_t, the bounded SER expression for GFDM based MRT system with multiple antennas is given in [24];

$$P_{SER,Nak} = 2C_1 C_2^{mN_t} C_4 \, {}_2F_1\left[mN_t, mN_t+\frac{1}{2}; mN_t+1; -C_3\right] - C_1^2\left[1 - \frac{4}{\pi}\sum_{j=0}^{mN_t-1} \frac{C_3^j}{2j+1} \, {}_2F_1\left[j+\frac{1}{2}, j+1; j+\frac{3}{2}; -(C_3+1)\right]\right] \tag{35}$$

where C_3 and C_4 are expressed as follows

$$C_3 = \frac{mN_t}{\overline{\gamma}_n}, \; C_4 = \frac{\Gamma\left(mN_t+\frac{1}{2}\right)}{\sqrt{\pi}\Gamma(mN_t+1)} \tag{36}$$

$$\overline{\gamma}_n = \frac{3R_T P_t N_t \sigma_n^2}{(2^\mu-1)} \frac{E_s}{\xi N_0} \tag{37}$$

In the above eq. (33), $\bar{\gamma}_n$ is equivalent to SNR in the Nakagami-fading environment. It is assumed that σ_n^2 value is 0.5. If we substitute m = 1 for both single and multiple antennas cases, the expressions give the SER expressions for the Rayleigh fading environment. For *m*=1, our simulation (Fig.2) is exactly matching with the simulation (Fig.2) given in [24]. For $N_t = 1$, eq. (33) and eq. (35) are exactly match with each other. For m = 1and K = 0, eq. (25) and eq. (33) gives the same results and those two equations merge to Rayleigh's fading environment.

5 Weibull Fading Environment

The modified PDF expression for the Rician fading environment is given in [34];

$$P_\gamma(\gamma) = \left(\frac{v}{2(a\overline{\gamma})^{\frac{v}{2}}}\right) \gamma^{\frac{v}{2}-1} \, exp\left(-\left(\frac{\gamma}{a\overline{\gamma}}\right)^{\frac{v}{2}}\right) \tag{38}$$

Now, SER expression for Weibull fading can be computed by substituting equ. (20) and equ. (38) in equ. (22), the bounded SER expression for GFDM system with single antenna is [33];

where $a = 1/\Gamma(1 + 2/v)$.

$$P_{Wbl}(e) = \frac{2(p-1)}{p}\frac{\frac{v}{2}}{(a\overline{\gamma})^{\frac{v}{2}}} I_3(\overline{\gamma}_{wb}) - \left(\frac{p-1}{p}\right)^2 \frac{\frac{v}{2}}{(a\overline{\gamma})^{\frac{v}{2}}} I_4(\overline{\gamma}_{wb}) \quad (39)$$

Where

$I_3(\overline{\gamma}_{wb})$ and $I_4(\overline{\gamma}_{wb})$ are expressed as given below;

$$I_3(\overline{\gamma}_{wb}) = \int_0^{\infty} \gamma^{\frac{v}{2}-1} e^{-\frac{\gamma^{\frac{v}{2}}}{(a\overline{\gamma_{wb}})^{\frac{v}{2}}}} erfc(\sqrt{\gamma}) d\gamma \quad (40)$$

$$I_4(\overline{\gamma}_{wb}) = \int_0^{\infty} \gamma^{\frac{v}{2}-1} e^{-\frac{\gamma^{\frac{v}{2}}}{(a\overline{\gamma_{wb}})^{\frac{v}{2}}}} erfc^2(\sqrt{\gamma}) d\gamma \quad (41)$$

Where

$$\overline{\gamma}_{wb} = \frac{3R_T\sigma_{wb}^2}{(2^{\mu}-1)}\frac{E_s}{\xi N_0} \quad (42)$$

From [33], $I_3(\overline{\gamma}_{wb})$ and $I_4(\overline{\gamma}_{wb})$

$$I_3(\overline{\gamma}_{wb}) = \frac{2(a\overline{\gamma}_{wb})^{\frac{v}{2}}}{v} - \frac{\left(\frac{k}{\lambda}\right)^{\frac{1}{2}}(\lambda)^{\frac{v}{2}}}{\sqrt{\pi}(2\pi)^{\frac{\lambda+k-2}{2}}} G_{2\lambda,k+\lambda}^{k+\lambda,\lambda}\left[\frac{\lambda^{\lambda}k^{-k}}{(a\overline{\gamma_{wb}})^{\frac{vk}{2}}} \middle| \begin{matrix} \Delta\left(\lambda, \frac{1-v}{2}\right),\ \Delta\left(\lambda, 1-\frac{v}{2}\right) \\ \Delta(k,0)\ ,\ \Delta\left(\lambda, \frac{-v}{2}\right) \end{matrix}\right] \quad (43)$$

$$I_4(\overline{\gamma}_{wb}) = \frac{2(a\overline{\gamma}_{wb})^{\frac{v}{2}}}{v}\left[1 - \frac{2}{\pi}\sum_{i=0}^{\infty}\frac{(-1)^i}{i!}\frac{\left(\frac{k}{\lambda}\right)^{\frac{1}{2}}(\lambda)^{\frac{i-1}{2}}}{\sqrt{\pi}(2\pi)^{\frac{\lambda+k-2}{2}}} G_{2\lambda,k+\lambda}^{k,2\lambda}\left[\frac{\lambda^{\lambda}k^{-k}}{(a\overline{\gamma_{wb}})^{\frac{vk}{2}}} \middle| \begin{matrix} \Delta\left(\lambda, \frac{1}{2}-i\right),\ \Delta(\lambda,-i) \\ \Delta(k,0)\ ,\ \Delta\left(\lambda,-i-\frac{1}{2}\right) \end{matrix}\right]\right] \quad (44)$$

Similarly, for multiple antennas (N_t) case, SER expression for GFDM based MRT system is obtained by changing K to KN_t.

4. Simulation Analysis

This section discusses the simulation results and their analysis. All the simulations are performed with simulation values such as number of subcarriers K= 64, length of CP N_{CP}= 8 and length of N_{Cs}= 0.

4.1 Specifications used for simulation

Parameter	Variable	Value
Modulation Scheme	μ(Modulation Index)	QPSK , 16-QAM
Sub-carriers	K	64
Block-length	M	16
Filter type	-	RRC
Roll-off factor	α	0.1,0.6,0.9
Channel	h(n)	1, for AWGN
Cyclic prefix	CP	-
Fading Channels	-	Rician, Weibull
Fading Parameter	K	0,1,2,3 If K=0 Channel is Rayleigh fading K= ∞ Channel is AWGN
Transmitting Antennas	N_t	4

Fig. 2 represents the SER analysis of GFDM-MRT based system for various values of SNRs using multiple antennas at the transmitter (N_t = 1,2,3,4) and with a roll-off factor α = 0.1. From the simulation, it is observed that simulation is evaluated for Rayleigh fading (K = 0) environment which is a special case of Rician fading with Rician fading parameter K= 0. It is also observed that SER performance decreases as the number of antennas increases.In[24] SER performance was calculated for only N_t=1 ,the value of SER is $0.13 * 10^{-2}$but in this paper we calculate SER performance for $N_t = 1, 2, 3$.For a particular case at SNR = 15dB, SER values are $0.13 * 10^{-2}$, $0.09 * 10^{-3}$,$0.66 * 10^{-4}$ and $0.03 * 10^{-5}$ for $N_t = 1, 2, 3, 4$ respectively. At $N_t = 4$ SER performance is compared with N_t=1 in[24] minimized the SER to 99.97%.Finally, it can be concluded that the GFDM-MRT scheme with $N_t = 4$ gives 10dB, 4dB, and 2dB SNR gain for $N_t = 1, 2, 3$ transmit antennas at SER=10^{-2}. Fig. 2 also compares the simulation results of [24] for different values of N_t, $K = 0$, and $\alpha = 0.1$

Fig. 3 represents the SER analysis of GFDM-MRT based system for various values of SNRs using multiple antennas at the transmitter ($N_t = 2$), various Rician fading parameters $K = (0,1,2,3)$ and with a roll-off factor α = 0.1. The curve for $K = 0$ is exactly matches with Rayleigh fading conditions and gives the same SER performance which matches with previous work [24]. But here, we can infer that as an increase in Rician fading parameter (K) from 0 to 3, the SER decreases.

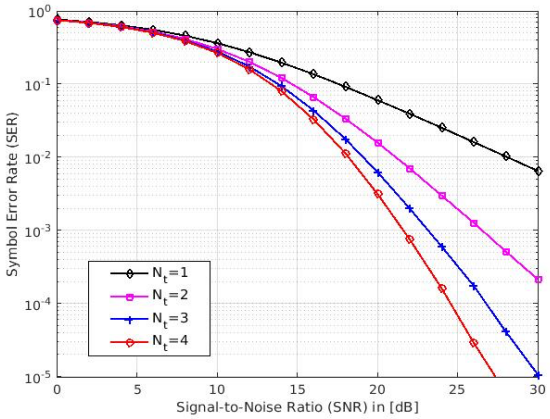

Fig. 2. SER vs SNR performance with the various number of transmitting antennas.

For a particular case at SNR=15dB, the error values for K= 0, 1, 2, 3 are respectively 0.01596, 0.0103, 0.0060 and 0.003. At K= 4 SER performance is compared with K=0[24] i.e. approximately there is an 81.2% decrease in error from K = 0 to K = 3. Finally, it can be concluded that GFDM-MRT scheme with $N_t = 4$ gives 10dB, 4dB, and 2dB SNR gain for $N_t = 1, 2, 3$ transmit antennas at SER=10^{-2}.

Fig. 4 is drawn between SER and SNR for different roll-off factors ($\alpha = 0.1, 0.6, 0.9$), $N_t = 2$, $K = 2$ and using a 16-QAM modulation scheme. Fig. 4 also explains the effect of the NEF parameter ξ which plays a key role in GFDM. As the value of the roll-off factor increases from 0.1 to 0.9, there is a significant change in the SER curve because as ξ increases there is a wider overlap of the subcarriers which increases the NEF factor. The SER values are 0.0216, 0.0116, 0.0060 at SNR=20dB for various values of $\alpha = 0.9$, 0.6 and 0.1 respectively. Here as α value decreases from 0.9

to 0.1, the SER value decreases by 72% but in literature[24] SER decresed by 50% as α value decreases from 0.9 to 0.1

Fig. 5 is drawn between SER and roll-off factor for different SNR values (10dB, 15dB, 20dB),$N_t = 3, K = 3$ and using 16-QAM modulation scheme. From the simulation it is observed that as SNR value increases from 10dB to 20dB, SER value decreases from 0.277 to 0.001 at $\alpha = 0.4$, it shows that there is an almost 95% improvement in SER with the increase in SNR. At a lower α value, the SER value is lower and it increases at higher α values. Finally, it can be concluded that to achieve less symbol error rate lower value at α=0.1 and higher SNR=20dB values are always recommendable.

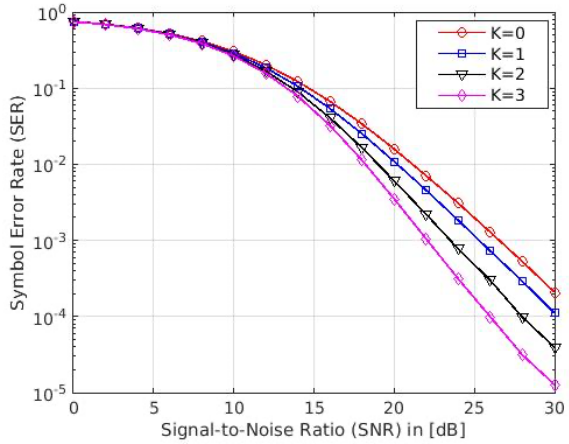

Fig. 3. SER vs SNR performance for various Rician fading parameters.

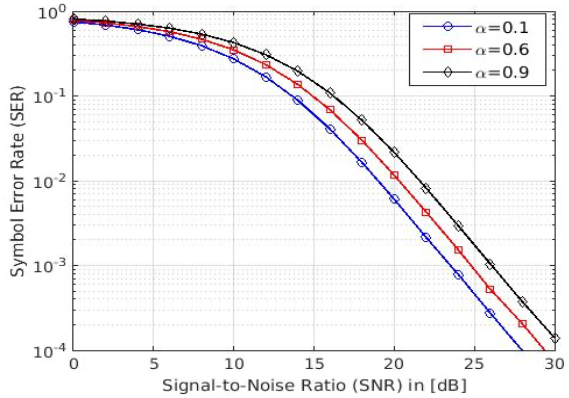

Fig.4. SER vs SNR performance for various Roll-off factors.

Fig. 6 is drawn between SER and SNRs for different modulation schemes (QPSK and 16-QAM),$K = 3$, $N_t = 3$ and $\alpha = 0.1$. From this simulation, we can state that the QPSK scheme achieves a lower value of SER compare to the 16-QAM modulation scheme. For a particular case, at SNR=10dB, SER values are 0.0251 and 0.0072 for 16-QAM and QPSK schemes.

Fig. 7 represents the SER performance of GFDM-MRT based system for various values of SNRs using multiple antennas at the transmitter ($N_t = 1,2,3,4$) and with a roll-off factor α = 0.1 under the Weibull fading channel.In literature [33] only at $N_t = 1$ transmitter SER performance analysed. It is observed from Fig.7 that SER performance falls as $N_t$increases. For a particular case at SNR= 15dB, SER values are 0.04409, 0.03329, 0.02054 and 0.01554 for $N_t = 1, 2, 3, 4$ respectively. Finally, it can be concluded that the GFDM-MRT scheme with $N_t = 4$ gives 4dB, 3dB, and 2dB SNR gain according to $N_t = 1, 2, 3$ transmit antennas respectively at SER=10^{-2}.

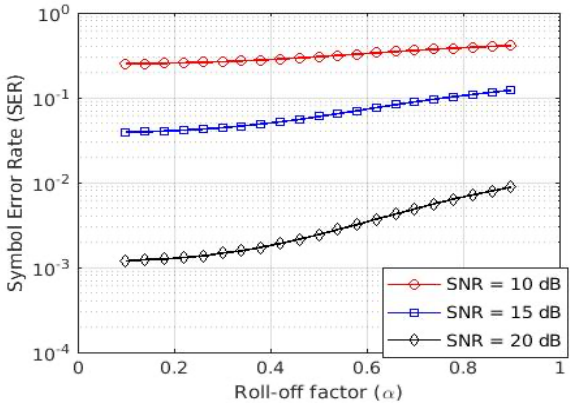

Fig. 5. SER vs roll-off factor for various SNR values.

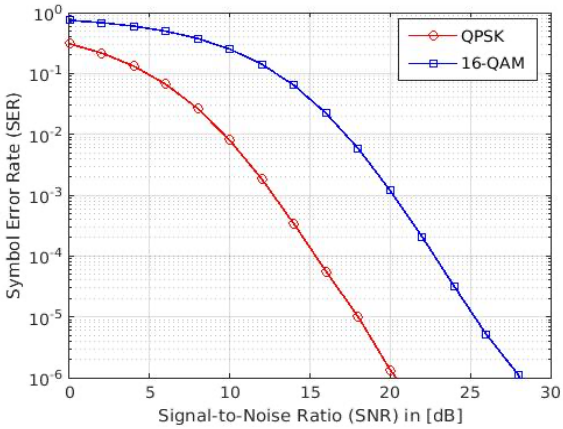

Fig.6. SER vs SNR performance for various modulation schemes.

Fig. 8 is drawn between SER and SNR for different roll-off factors ($\alpha = 0.1, 0.6, 0.9$), $N_t = 2$and using a 16-QAM modulation scheme. Fig. 8 also explains the effect of the NEF parameter ξ which plays an important role in GFDM. The SER values are 0.04064, 0.02054, 0.01129 at SNR=16dB for various values of $\alpha = 0.9$, 0.6 and 0.1 respectively. As α value decreases from 0.9 to 0.1, the SER value decreases by 72.2%.

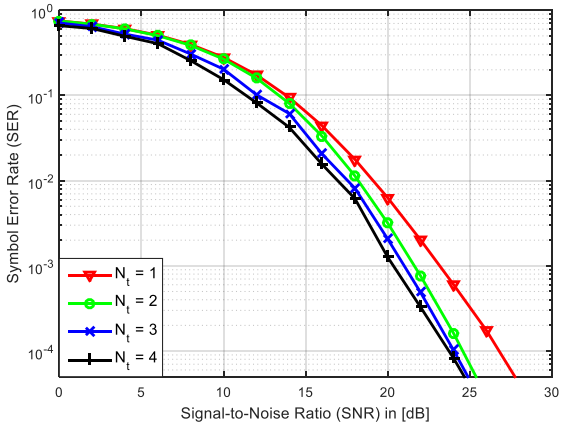

Fig.7. SER vs SNR performance with the various number of transmitting antennas.

Fig. 9 is drawn between SER and roll-off factor for different SNR values (10dB, 15dB, 20dB),$N_t = 3$ and using a 16-QAM modulation scheme. From the simulation, it is

observed that as SNR value increases from 10dB to 20dB, SER value decreases from 0.03525 to 0.05544 at $\alpha = 0.4$, which shows that there is an almost 57.2% improvement in SER with the increase in SNR. The SER value is less at lower values of α and it increases and is high at higher values of α.

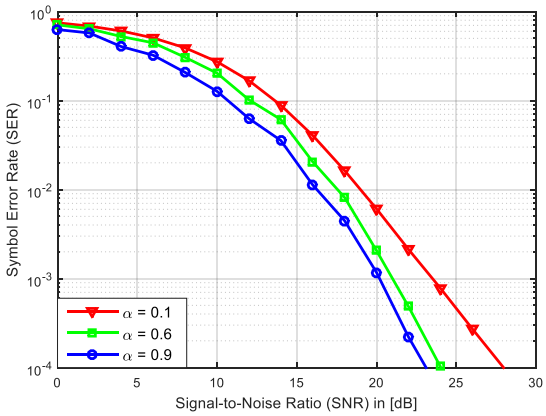

Fig.8. SER vs SNR performance for various Roll-off factors.

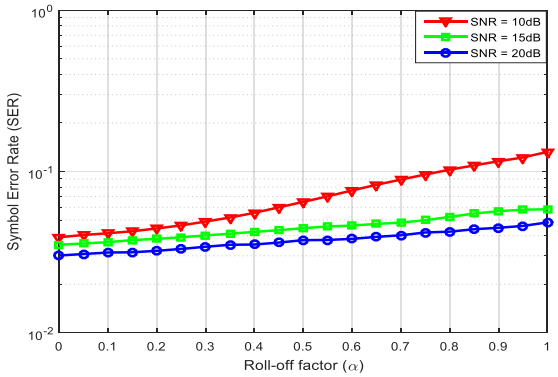

Fig.9. SER vs roll-off factor for various SNR values.

5. Conclusion

Under the Rician fading environment, the proposed GFDM-MRT scheme is suggested and its symbol error rate (SER) performance is investigated. Initially, the closed form of SER expression under Rician and Weibullfading environment for single and multiple antennas has provided. Later on, SER performance is evaluated with MATLAB simulations for various simulation parameters such as several transmitting antennas, different roll-off factors, and various fading parameters. We have also validated our simulations with the existing literature papers. The SNR performance is improved by approximately 6dB to achieve the symbol error rate of 0.01, when we use the number of transmitting antennas $(N_t = 4)$ compared to a single antenna. $(N_t = 1)$. Finally, it can be concluded that the GFDM-MRT technique is more reliable for high-speed communications.

References

1. A. Farhang, N. Marchetti, and L. Doyle, "Low Complexity Transceiver Design for GFDM", *IEEE Transactions on Signal Processing,* Vol. 64, Issue 6, pp.1507-1518, March-2016.
2. Z. Sharifian, M. Omidi, A. Farhang and H. Source, "Polynomial-Based Compressing andIterative Expanding for PAPR Reduction in GFDM", *23rd Iranian Conference on Electrical Engineering*, pp. 518-523, Iran, May-2015.
3. J. S. Ferreira, H. D. Rodrigues, A. A. Gonzalez, A. Nimr, M. Matthé, D. Zhang, L. L. Mendes, and G. Fettweis, "GFDM frame design for 5G application scenarios," *J. Commun. and Information Systems*, vol. 32, no. 1, pp. 54-61, 2017.
4. D. Zhang, M. Matthé, L. L. Mendes, and G. Fettweis, "A study on the link level performance of advanced multicarrier waveforms under MIMO wireless communication channels," *IEEE Trans. Wireless Commun*., vol. 16, no. 4, pp. 2350 - 2365, Mar. 2017.
5. N. Michailow, M. Matthé, I. S. Gaspar, A. N. Caldevilla, L. L. Mendes, A. Festag, and G. Fettweis, "Generalized frequency division multiplexing for 5th generation cellular networks," *IEEE Trans. Commun*., vol. 62, no. 9, pp. 3045-3061, Sep. 2014.
6. N. Michailow, L. Mendes, M. Matthe, I. Gaspar, A. Festag and G. Fettweis, "Robust WHTGFDM for the Next Generation of Wireless Networks", *IEEE Communications Letters*, Vol. 19, Issue 1, pp. 106-109, November-2014.
7. I. Gasper, L. Mendes, M. Matthe, N. Michailow, A. Festag and G. Fettweis, "LTE- Compatible 5G PHY based on Generalized Frequency Division Multiplexing", *in Proceedings of the 11th International Symposium on Wireless Communications Systems,*pp. 209-213, Spain, August-2014.
8. G. Fettweis, M. Krondorf, and S. Bittner, "GFDM – Generalized Frequency Division Multiplexing," *Vehicular Technology Conference*, 2009.
9. S. Antapurkar, Pandey and K. Gupta, "GFDM Performance in terms of BER, PAPR andOOB and comparison to OFDM system", *2nd International Conference on communication systems*, India, October-2015.
10. A. Kumar, M. Magarini, "Improved Nyquist Pulse Shaping Filters for Generalized Frequency Division Multiplexing", *IEEE Latin American Conference on Communications,* pp. 1-7, November 2016.
11. N. Michailow and G. Fettweis, "Low Peak-to-Average Power Ratio for Next Generation Cellular Systems with Generalized Frequency Division Multiplexing," *IEEE International Symp. on Int. Sig. Proc. and Comm. Sys.*, Nov. 2013, pp. 651-655.
12. N. Michailow, S. Krone, M. Lentmaier and G. Fettweis, "Bit Error Rate Performance of Generalized Frequency Division Multiplexing," *Vehicular Technology Conference*, 2012
13. R. Datta, N. Michailow, M. Lentmaier, and G. Fettweis, "GFDM Interference CancellationFor Flexible Cognitive Radio PHY Design," *Vehicular Technology The conference*, 2012.
14. S. Tiwari, S. S. Das, K. K. Bandyopadhyay, "Precoded generalized frequency division multiplexing system to combat inter-carrier interference: performance analysis," *IET Comm.*, vol. 9, no. 15, pp. 1829-1841, May. 2015.
15. M. Matthe, L. L. Mendes and G. Fettweis, "Space-Time Coding for Generalized frequency Division Multiplexing," *European Wireless Conference*, 2014.
16. M. Matthe, L. L. Mendes, N. Michailow, D. Zhang, and G. Fettweis, "Widely Linear Estimation for Space-Time-Coded GFDM in LowLatency Applications," *IEEE Transactions on Communications*, vol. 63, no. 11, pp. 4501-4509, Nov. 2015.

17. N. E. Tunali, M. Wu, C. Dick, and C. Studer, "Linear Large-Scale MIMO Data Detection for 5G Multi-Carrier Waveform Candidates," *Conference on Signals, Systems and Computers*, 2015.
18. J. Datta, H.-P.Lin, and D.-B. Lin, A method to implement interference avoidance based MIMO-GFDM using spatial modulation," *Inter. Conf. on Advanced Tech. for Comm.*,2015.
19. M. Matthe, I. S.Gaspar, D. Zhang, and G. Fettweis, "Near ML Detection" for MIMO-GFDM," *Vehicular Technology Conference*, 2015.
20. D. Zhang, M. Matthe, L. L. Mendes, and G. Fettweis, "A Markov Chain Monte Carlo Algorithm for Near-Optimum Detection of MIMOGFDM Signals," *Inter. Symp. onPersonal Indoor and Mobile Radio Communication*, 2015.
21. D. Zhang, M. Matth, L. L. Mendes, I. S.Gaspar, N. Michailow, and G. Fettweis, Expectation Propagation for Near-Optimum Detection of MIMO-GFDM Signals," *IEEE Trans. on Wireless Comm.*, vol. 15, no. 2, pp. 1045-1062, Feb. 2016.
22. T. K. Y. Lo, "Maximum ratio transmission," *IEEE Trans. on Comm.*, vol. 47, no. 10, pp. 1458-1461, 1999.
23. E. Erdogan, T. Gucluoglu, "Performance Analysis of Maximal Ratio Transmission with Relay Selection in Two-way Relay Networks Over Nakagami-m Fading Channels," *Wireless Personal Communications Journal*, 2015.
24. A. Yenilmez, T. Gucluoglu, and P. Remlein, "Performance of GFDM-maximal ratio transmission over Nakagami-m fading channels," *2016 International Symposium on Wireless Communication Systems (ISWCS)*, Poznan, 2016, pp. 523-527.
25. S. K. Bandari, A. Drosopoulos, V.V. Mani, "Exact SER Expressions of GFDM in Nakagami-m and Rician fading channels," *European Wireless Conference*, 2015.
26. J. W. Browning, S. L. Cotton, D. Morales-Jimenez and F. J. Lopez-Martinez, "The Rician Complex Envelope Under Line of Sight Shadowing," in *IEEE Communications Letters*, vol. 23, no. 12, pp. 2182-2186, Dec. 2019.
27. M. Simon and M. Alouini, *Digital Communication over Fading Channels*, 2nd ed. Hoboken, NJ: Wiley Interscience, John Wiley & Sons, 2005.
28. B. Sklar, *Digital Communications: Fundamentals and Applications*, 2nd ed. New York, NY, USA: Prentice-Hall, 2001.
29. I. Abramowitz, M. amdStegun, *Handbook of Mathematical Functions*. Dover, 1970.
30. I. Gradshteyn and I. Ryzhik, *Table of Integrals, Series, and Products*, 5th ed. Academic Press, 1994.
31. Cheng, J., Tellambura, C. and Beaulieu, N. (2003), "Performance analysis of digital modulations on Weibull fading channels", 58th Vehicular Technology Conference, VTC 2003-Fall, 2003 IEEE, Vol. 1, pp. 236-240.
32. Sagias, N., Karagiannidis, G., Zogas, D., Mathiopoulos, P. and Tombras, G. (2004), "Performance analysis of dual selection diversity in correlated Weibull fading channels", IEEE Transactions on Communications, Vol. 52 No. 7, pp. 1063-1067.
33. Bandari, S.K., Mani, V.V. and Drosopoulos, A. (2016), "Performance analysis of GFDM in various fading channels", COMPEL - The international journal for computation and mathematics in electrical and electronic engineering, Vol. 35 No. 1, pp. 225-244.
34. Nalgonda, S., Bandari, S.K., Dhar Roy, S. and Kundu, S, "On the performance of weighted fusion-based spectrum sensing in fading channels", Journal of Computational Engineering, Vol.10, 2013.